

Short communication

Microstructure evolution of Ti_3SiC_2 powder during high-energy ball millingLeifeng Liu^a, Lianjun Wang^{b,*}, Lu Shi^a, Wan Jiang^{a,b,**}^a State Key Laboratory of High Performance Ceramics and Superfine Microstructure, Shanghai Institute of Ceramics, Chinese Academy of Sciences, 1295 Dingxi Road, Shanghai 200050, People's Republic of China^b State Key Laboratory for Modification of Chemical Fibers and Polymer Materials, Donghua University, Shanghai 201620, People's Republic of China

Received 31 July 2009; received in revised form 11 February 2010; accepted 2 April 2010

Abstract

Ti_3SiC_2 powder was milled by high-energy ball milling under argon atmosphere and subsequently thermally annealed. The microstructure evolution of Ti_3SiC_2 after milling was investigated. It was found that 200 nm particle size Ti_3SiC_2 powder could be achieved by 9 h milling whereas a longer milling time would induce Ti_3SiC_2 decomposition. After 18 h milling, the particle size gradually decreased to 150 nm and TiC appeared in the XRD pattern. It is suggested that the collision of the milling balls triggered the formation of TiC from the amorphous phase which was generated in the milling process.

© 2010 Elsevier Ltd and Techna Group S.r.l. All rights reserved.

Keywords: High-energy ball milling; Ti_3SiC_2 ; Nanopowder

1. Introduction

Titanium silicon carbide (Ti_3SiC_2) has attracted much attention due to its special nanolaminated microstructure and unique properties combining the advantages of both ceramic and metal [1,2]. It has a hexagonal structure in which every three nearly closed-packed Ti layers with the C atoms in the octahedral sites between them are separated by hexagonal nets of Si atoms [3–5]. Like ceramics, Ti_3SiC_2 possesses low density (4.52 g cm^{-3}), excellent high-temperature mechanical properties, high melting point and thermal stability. Like metal, Ti_3SiC_2 is relatively soft (H_V : 4 GPa), machinable, damage tolerant, resistant to thermal shock and shows good electrical and thermal conductivities (being about $4.5 \times 10^6 \Omega^{-1} \text{ m}^{-1}$ and $37 \text{ W m}^{-1} \text{ K}^{-1}$) [6,7].

Due to these outstanding properties, a lot of work has been done in the fabrication of advanced Ti_3SiC_2 -toughened and Ti_3SiC_2 -based composites, including $\text{Al}_2\text{O}_3/\text{Ti}_3\text{SiC}_2$, $\text{Ti}_3\text{SiC}_2/$

TiC, $\text{Ti}_3\text{SiC}_2/\text{SiC}$ and others [8–14]. It is well known grain size to have a dramatic effect on the mechanical properties of materials. In most of the studies, the grain size of Ti_3SiC_2 in the bulk materials is in the range of a few or a few tens of micrometers. If the grain size of Ti_3SiC_2 can be reduced to nanosize, the mechanical properties might be improved substantially.

High-energy ball milling is a solid-state powder processing technique involving repeated welding, fracturing, and rewelding of powder particles [15]. Since it was first proposed by Benjamin in 1970, high-energy ball milling has been proved to be a powerful technique to prepare new and advanced materials including nanocrystalline powders, nanopowders, intermetallic powders, amorphous alloys, and others [16,17].

In this paper, high-energy ball milling was employed for refinement of coarse Ti_3SiC_2 powder. The microstructure evolution of Ti_3SiC_2 powder after the high-energy ball milling was investigated.

2. Experimental

Titanium, graphite, silicon and aluminum powders mixed in the molar ratio of 3:2:1.2:0.2 were used to synthesize Ti_3SiC_2 powder employing a spark plasma sintering apparatus (SPS-2040, Sumitomo Coal Mining Co., Tokyo, Japan) at 1280°C under argon atmosphere. Then the Ti_3SiC_2 powder was milled

* Corresponding author. Tel.: +86 21 52412550.

** Corresponding author at: State Key Laboratory of High Performance Ceramics and Superfine Microstructure, Shanghai Institute of Ceramics, Chinese Academy of Sciences, 1295 Dingxi Road, Shanghai 200050, People's Republic of China. Tel.: +86 21 52411118; fax: +86 21 52413122.

E-mail addresses: wanglj@dhu.edu.cn (L. Wang), wangjiang@mail.sic.ac.cn (W. Jiang).

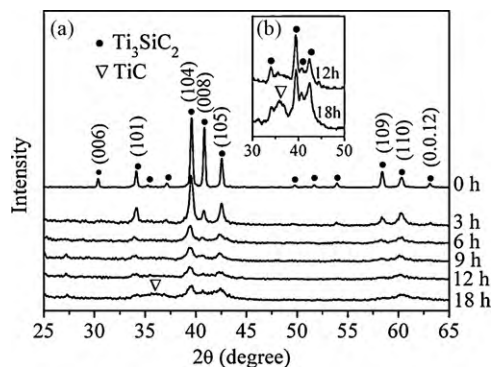


Fig. 1. XRD patterns of (a) the unmilled powder and the powders milled for different times and (b) the powder after 12 h and 18 h milling.

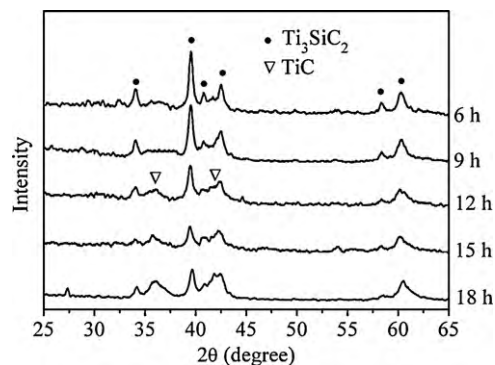


Fig. 2. XRD patterns of the powders milled for different times and then annealed at 800 °C for 12 h.

in a high-energy ball milling machine (Model GN-2, Shenyang Science Equipment Factory, Shenyang, China) at the speed of 480 rpm using a steel vial of 60 mm inner diameter and a series of hardened steel balls 6.5 mm, 8.5 mm and 9.5 mm in diameter. The ball-to-powder weight ratio was 13:1, and the steel vial was sealed in a glove box under argon atmosphere. During the process, the milling was paused periodically to collect a small amount of the powders for analysis and post treatment. The powders milled for various times were then annealed in vacuum at 800 °C for 12 h.

The powders synthesized, milled and annealed were analyzed by X-ray diffraction (XRD) with Cu K α radiation at 40 kV and 100 mA. Particle morphology and microstructure observation were performed by scanning electron microscopy (SEM) and transmission electron microscopy (TEM).

3. Results and discussion

The XRD patterns of unmilled Ti_3SiC_2 powder and the powders milled for different times are shown in Fig. 1a. For

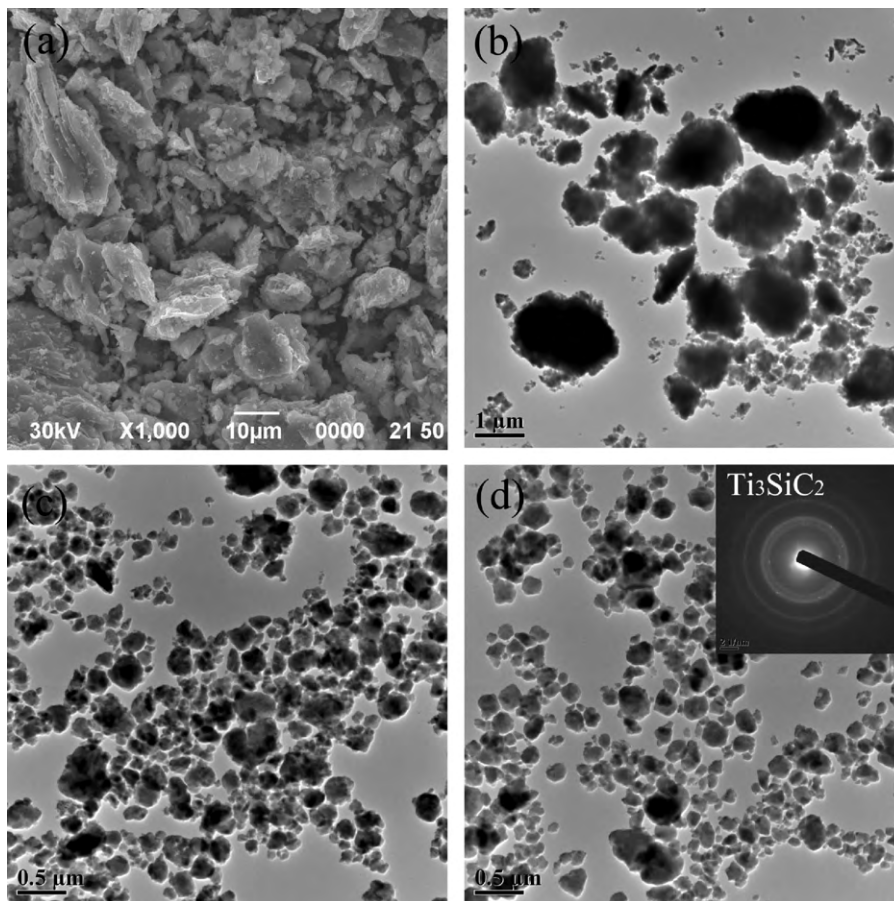


Fig. 3. (a) SEM image of the unmilled powder and TEM images of the powder milled for (b) 3 h, (c) 9 h and (d) 18 h with the corresponding electron diffraction pattern.

unmilled powder, no reflection of impurities was detected in the X-ray profile, i.e. single-phase Ti_3SiC_2 powder was achieved. The reflections of Ti_3SiC_2 broadened with the increase of the milling time, due to the decrease of the grain size and the increase of the lattice strain during milling. The lowering of intensity of Ti_3SiC_2 reflections together with the increase in background shows evidence that a part of crystalline Ti_3SiC_2 transformed to amorphous phase during the high-energy milling process. The formation of the amorphous phase is also confirmed by the significant broadened diffraction ring of Ti_3SiC_2 powder milled for 18 h (Fig. 3d). It was worth to note that the intensity of the (0 0 8) peaks of Ti_3SiC_2 (basal planes reflection), decreased much faster than other peaks. Owing to the hugely anisotropic structure with lattice parameters $a = 0.307$ nm and $c = 1.77$ nm, the resistance of the Ti_3SiC_2 grains to shear on non-basal planes is much greater than that on basal planes [1,4]. During milling, the vast majority of dislocations occur on the basal plane leading to the decrease of the long-range lattice order in the direction of c -axis. As a result, the XRD reflections of the basal plane weakened much faster than others.

Fig. 1b confirms the XRD patterns of the Ti_3SiC_2 powders milled for 12 h and 18 h. Showing the TiC reflections at $2\theta = 36.013^\circ$ to appear in the latter pattern, i.e. part of Ti_3SiC_2 powder decomposed when milled for 18 h. Ti_3SiC_2 is stable to at least 1700°C in inert atmosphere [3,10]. At temperature $>1700^\circ\text{C}$, decomposition of Ti_3SiC_2 occurs through the removal of Si from the structure and the related detwinning of the Ti_3SiC_2 layers to form TiC [18]. In the present experiment, the local temperature could rise to only a few hundred degree Celsius for a very short time, i.e. at a much lower level than the decomposition temperature of Ti_3SiC_2 . Hence, a different decomposition mechanism shall occur. It is supposed that triggered by the collision of milling balls, the TiC grains nucleate and grow within the amorphous phase generated after long time milling.

The Ti_3SiC_2 powders milled for different times were annealed at 800°C for 12 h in vacuum to recrystallize the amorphous phase. The XRD patterns of annealed powders (Fig. 2) show that TiC began to nucleate after milling time up to 12 h. Due to the limited amount of TiC, its reflections could hardly be detected by XRD. The TiC grain grew and a large amount of amorphous phase transformed to TiC in the subsequent annealing, which made its reflections distinct in the XRD pattern in Fig. 2. Intermetallics of Ti and Si, such as TiSi_2 and Ti_5Si_3 , might also form. However, being the TiSi_2 and Ti_5Si_3 reflections very close to the ones of Ti_3SiC_2 , it is difficult to identify them in the XRD patterns.

The SEM images of the powders milled for different times are shown in Fig. 3a–d. Before milling, the particle size of the Ti_3SiC_2 powder was from a few μm to a few tens of μm . At the beginning of the milling, the average particle size in the observed region decreased rapidly by deformation and fragmentation mechanism to about $1.5\ \mu\text{m}$ after 3 h milling and to about $200\ \text{nm}$ after 9 h milling. When the milling time was up to 18 h, the particle size declined more slowly to about $150\ \text{nm}$, possibly due to coalescence [17]. The significant

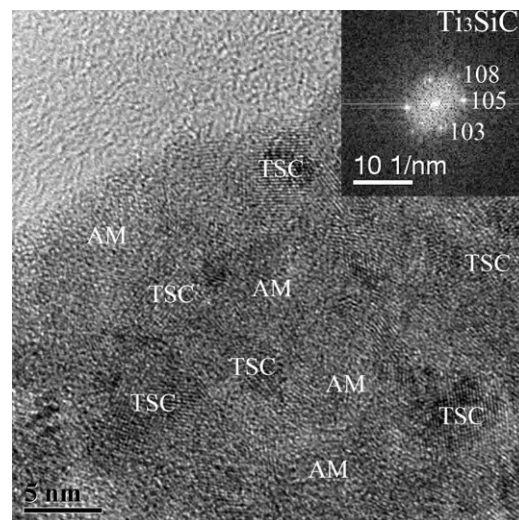


Fig. 4. High resolution TEM micrograph of Ti_3SiC_2 powder milled for 18 h (TSC, Ti_3SiC_2 ; AM, amorphous region).

broadening of the diffraction ring in the diffraction pattern shown in Fig. 3d confirms that a large amount of amorphous phase appeared after 18 h milling.

Fig. 4 shows a high resolution transmission electron microscopy (HRTEM) micrograph of the Ti_3SiC_2 powder milled for 18 h. The fast Fourier transform (FFT) method was applied to correlate the lattice distances of the individual crystallites with corresponding standard phases. Crystalline Ti_3SiC_2 with grain size of a few nanometers separated in the powder particle where a considerable amount of amorphous phase was also detected.

4. Conclusions

During the high-energy ball milling of Ti_3SiC_2 powder, the particle size was found to decrease rapidly at the early milling stage, from $8\ \mu\text{m}$ before milling to about $200\ \text{nm}$ after 9 h milling and then to decrease slightly to about $150\ \text{nm}$ after 18 h milling. Presence of TiC possibly nucleated from the amorphous phase indicates decomposition of Ti_3SiC_2 to start after 12 h milling. Hence, high purity $200\ \text{nm}$ Ti_3SiC_2 powder could be achieved by 9 h milling.

Acknowledgements

This work was funded by Natural Science Foundation of China (Nos. 50625414, 50821004 and 50954002), Program of Shanghai Subject Chief Scientist (No. 08XD14046), Shanghai Rising-Star Program (No. 09QA1406600) and Shanghai Nano Science and Technology Special Project (No. 0852nm03300).

References

- [1] M.W. Barsoum, M. Radovic, P. Finkel, T. El-Raghy, Ti_3SiC_2 and ice, Appl. Phys. Lett. 79 (2001) 479–481.
- [2] H.B. Zhang, Y.W. Bao, Y.C. Zhou, Current status in layered ternary carbide Ti_3SiC_2 , a review, J. Mater. Sci. Technol. 25 (2009) 1–38.

- [3] M.W. Barsoum, T. El-Raghy, Synthesis and characterization of a remarkable ceramic: Ti_3SiC_2 , *J. Am. Ceram. Soc.* 79 (7) (1996) 1953–1956.
- [4] M. Zakeri, M.R. Rahimipour, A. Khanmohammadian, Effect of the starting materials on the reaction synthesis of Ti_3SiC_2 , *Ceram. Int.* 35 (2009) 1553–1557.
- [5] Z.F. Zhang, Z.M. Sun, H. Hashimoto, Fabrication and microstructure characterization of Ti_3SiC_2 synthesized from Ti/Si/2TiC powders using the pulse discharge sintering (PDS) technique, *J. Am. Ceram. Soc.* 86 (3) (2003) 431–436.
- [6] Y. Zou, Z.M. Sun, S. Tada, H. Hashimoto, Effect of liquid reaction on the synthesis of Ti_3SiC_2 powder, *Ceram. Int.* 34 (2008) 119–123.
- [7] T. El-raghy, M.W. Barsoum, Processing and mechanical properties of Ti_3SiC_2 : I. reaction path and microstructure evolution, *J. Am. Ceram. Soc.* 82 (10) (1999) 1854–2849.
- [8] D.T. Wan, Y.W. Bao, J.Z. Peng, Y.C. Zhou, Fracture toughness determination of $\text{Ti}_3\text{Si}(\text{Al})\text{C}_2$ and Al_2O_3 using a single gradient notched beam (SGNB) method, *J. Eur. Ceram. Soc.* 29 (2009) 763–771.
- [9] Y.M. Luo, S.Q. Li, J. Chen, R.G. Wang, J.Q. Li, W. Pan, Effect of composition on properties of alumina/titanium silicon carbide composites, *J. Am. Ceram. Soc.* 85 (12) (2002) 3099–3101.
- [10] J.F. Zhang, L.J. Wang, W. Jiang, L.D. Chen, Effect of TiC content on the microstructure and properties of Ti_3SiC_2 –TiC composites in situ fabricated by spark plasma sintering, *Mater. Sci. Eng. A* 487 (2008) 137–143.
- [11] Y.M. Luo, W. Pan, S.Q. Li, R.G. Wang, J.Q. Li, Fabrication of Al_2O_3 – Ti_3SiC_2 composites and mechanical properties evaluation, *Mater. Lett.* 57 (2003) 2509–2514.
- [12] C.F. Hu, Y.C. Zhou, Y.W. Bao, D.T. Wan, Tribological properties of polycrystalline Ti_3SiC_2 and Al_2O_3 -reinforced Ti_3SiC_2 composites, *J. Am. Ceram. Soc.* 89 (11) (2006) 3456–3461.
- [13] J.F. Zhang, L.J. Wang, L. Shi, W. Jiang, L.D. Chen, Rapid fabrication of Ti_3SiC_2 –SiC nanocomposite using the spark plasma sintering-reactive synthesis (SPS-RS) method, *Scripta Mater.* 56 (2007) 241–244.
- [14] Q.F. Zan, L.M. Dong, C. Wang, C.A. Wang, Y. Huang, Improvement of mechanical properties of $\text{Al}_2\text{O}_3/\text{Ti}_3\text{SiC}_2$ multilayer ceramics by adding SiC whiskers into Al_2O_3 layers, *Ceram. Int.* 33 (2007) 385–388.
- [15] C. Suryanarayana, Mechanical alloying and milling, *Prog. Mater. Sci.* 46 (2001) 1–184.
- [16] S.F. Liu, L.G. Zhang, L.N. An, Phase transformation of mechanically milled nano-sized γ -alumina, *J. Am. Ceram. Soc.* 88 (9) (2005) 2559–2563.
- [17] Y.S. Kwon, P.P. Choi, J.S. Kim, D.H. Kwon, K.B. Gerasimov, Decomposition of intermetallics during high-energy ball-milling, *Mater. Sci. Eng. A* 449–451 (2007) 1083–1086.
- [18] M.W. Barsoum, The $\text{M}_{N+1}\text{AX}_N$ phases: a new class of solids; thermodynamically stable nanolaminates, *Prog. Solid. State Chem.* 28 (2000) 201–281.